

Lung ultrasound predicts histological lung injury in a neonatal model of acute respiratory distress syndrome

Yasser N. Elsayed MD, PhD¹ | Martha Hinton MSc² | Ruth Graham MD³ |
Shyamala Dakshinamurti MD, MSc^{1,2,4} 

¹Department of Pediatrics, Section of Neonatology, University of Manitoba, Winnipeg, Canada

²Biology of Breathing Theme, Children's Hospital Research Institute of Manitoba, Winnipeg, Canada

³Department of Anesthesia, University of Manitoba, Winnipeg, Canada

⁴Department of Physiology, University of Manitoba, Winnipeg, Canada

Correspondence

Shyamala Dakshinamurti, MD, MSc, University of Manitoba, Section of Neonatology, Women's Hospital, WN 2618 – 820 Sherbrook St, Winnipeg R3A1R9, Canada.
Email: shyamala.dakshinamurti@umanitoba.ca

Funding information

University of Manitoba Department of Anesthesia; Winnipeg Rh Institute Foundation; Heart and Stroke Foundation of Canada, Grant/Award Number: G190024330

Abstract

Rationale: Point-of-care ultrasound (POCUS) is used to evaluate pulmonary edema in adults with acute respiratory distress syndrome (ARDS). Its use has not been validated in neonatal models.

Objectives: We compared an in vivo lung ultrasound score against clinical and histological markers of acute lung injury, in a neonatal animal model, hypothesizing that POCUS would sensitively diagnose early acute lung injury in neonates and discern its severity.

Methods: Fifteen anesthetized, ventilated 3-day-old neonatal piglets were divided into controls, moderate lung injury, or severe lung injury by graded treatment with oleic acid. Degree of lung injury was quantified at baseline, immediately after oleic acid administration, and 1 hour after the evolution of acute lung injury, by blood gases, ventilation parameters and calculated oxygenation deficit; hemodynamic indices by echocardiography, and lung ultrasound obtained in an 8-region grid of anterior and posterior zones, semi-quantitatively analyzed by a blinded observer. Lungs were inflation-fixed postmortem at last mean airway pressure, for histological assessment.

Results: Acute lung injury manifested in oleic acid-treated groups as dose-dependent capillary leak causing intravascular depletion and cardiac failure, hypoxemia with increasing intrapulmonary shunt fraction, decreased lung compliance, and resistance. Ultrasound scores of anterior regions distinguished moderate from severe injury; scores in posterior regions reached maximum values immediately after lung injury. POCUS score correlated with calculated intrapulmonary shunt fraction ($R^2 = .65$) and with histological injury score ($R^2 = .61$), $P < .01$.

Conclusion: We conclude that POCUS may be valuable in neonates for early quantification of acute lung injury or ARDS; and that nondependent ultrasound regions clearly distinguish severity of pulmonary edema.

KEYWORDS

acute respiratory distress syndrome, neonatal lung, oleic acid lung injury, point-of-care lung ultrasound

1 | INTRODUCTION

Point-of-care lung ultrasound (POCUS) is commonly used in the newborn and adult intensive care unit, to identify the presence of pneumonia, pulmonary edema, or lung injury.¹ Its ability to discern the magnitude of acute lung injury (ALI) has not been systematically studied, especially in a neonatal population. The aim of this study was to determine how closely a blinded lung ultrasound (US) score correlates with the degree of ALI, as quantified clinically and histologically, in a neonatal animal model.

Acute respiratory distress syndrome (ARDS) complicates the systemic inflammatory response of sepsis, including many viral infections. It is characterized by uncontrolled proinflammatory cytokine activation, diffuse epithelia and endothelial injury-causing permeability edema, hypoxemia, and poorly compliant lungs²; and is notoriously difficult to model, due to animal instability and high mortality.³ ALI induced by oleic acid (OA) in pigs is a stable, reproducible model⁴ that recreates the early, direct endothelial injury and pulmonary edema phase of ARDS, 1 minute postinjection.⁵ We have used this model extensively to examine mechanical ventilation modes, potential treatment modalities,^{6–8} and to assess recruitment with computed tomography (CT) imaging⁹ in juvenile and adult pigs, but neonatal parallels are lacking.

Neonatal ARDS was redefined by the Montreux consensus in 2017 as extensive lung inflammation of acute onset triggered directly by lung injury, or indirectly by an extrapulmonary process such as sepsis, asphyxia, or inflammation, resulting in qualitative or quantitative surfactant dysfunction. Clinical manifestations include decreased lung compliance, heterogeneous atelectasis, intrapulmonary right-to-left shunt, ventilation-perfusion mismatch, and hypoxemia.¹⁰ Diagnostic criteria include the bilateral presence of diffuse, irregular pulmonary opacities, or infiltrates, as well as noncardiogenic pulmonary edema and (preductally measured) oxygenation deficit.¹⁰ Typically this diagnosis requires chest radiography; the substitution of lung US has been robustly debated.^{11,12} While POCUS is used to semi-quantitatively follow lung aeration,¹³ it is not yet recommended for evaluation of ARDS severity in neonates,¹ due to limited concordance between chest radiography and lung US. However, X-ray is not a sine qua non; we submit that neonatal lung US should be assessed more rigorously by comparison to a tissue-based gold standard and clinical indices.

In this study, we induced a graded degree of ALI in neonatal piglets using OA, and compared blinded lung US scores with detailed histological evaluation of lung injury using standardized criteria. Blood gas, ventilation, and echocardiographic evaluations permitted assessment of pulmonary and cardiovascular consequences during the evolution of ARDS in this neonatal model. We hypothesized that lung US would prove more sensitive than contemporaneous clinical observation, and would track closely with histological severity of lung injury.

2 | METHODS

The experimental protocol (Figure 1) was approved by the University of Manitoba Animal Ethics committee per Canadian Council on Animal Care guidelines. Healthy newborn piglets (*Sus scrofa familiaris*)

were obtained from a pathogen-free farm supplier at 3 days age. Animals were sedated with ketamine/xylazine and atropine, followed by inhalational induction with 8% sevoflurane before intubation, then maintained on a continuous infusion of propofol and ketamine to minimize inhalational anesthesia-associated cardiovascular depression, and paralyzed with rocuronium. Continuous mechanical ventilation was initiated in assist control volume guarantee mode with tidal volume (TV) 6 mL/kg, positive end-expiratory pressure (PEEP) 6 cm H₂O, FiO₂ 50%, Ti 0.3, and the rate adjusted to maintain arterial partial pressures of carbon dioxide (PaCO₂) within a normal range. Airway pressure, flow, and TV were measured by neonatal pneumotach. Femoral arterial, venous, and external jugular cannulae were placed via cutdowns. Electrocardiograph, arterial blood pressure, central venous pressure, peripheral O₂ saturation, and core temperature were continuously monitored; normothermia was maintained by a heating blanket.

Animals were stabilized for 15 minutes after placement of lines. *Baseline* assessment included arterial and venous blood gas samples, and respiratory system mechanics determined from continuously recorded airway pressure and volume loops. *Baseline* cardiovascular hemodynamics included heart rate (HR), mean arterial (mBP), and central venous blood pressures (CVP). Functional echocardiography¹⁴ and POCUS scores were obtained at baseline, immediately following lung injury induction, and after 1 hour equilibration of lung injury, using GE Vivid e9 machine with 12 MHz high frequency probe. Pulmonary aeration was imaged in the supine position as three anterior regions and one posterior US region for each lung.¹⁵ Echocardiogram and US images were analyzed by an investigator blinded to treatment group assignment (YE) and scored following standardized criteria. Details of echocardiography and lung US provided in Methods supplement.

Animals were randomized to receive control, moderate injury, or severe injury, by intravenous injection of OA or diluent. OA emulsified in 2 mL normal saline was infused via jugular venous catheter; moderate injury animals received 0.2 mL/kg OA over 20 minutes, severe injury animals received a second dose of 0.1 to 0.2 mL/kg as tolerated by ventilation and hemodynamics. Dopamine up to 10 µg/kg/min was infused to support hemodynamics during OA administration. After administration, animals were stabilized for 15 minutes off dopamine, followed by *Post Treatment* blood gases, respiratory mechanics, and lung US. Animals were then maintained for 1 hour for the evolution of their lung injury to a stable plateau, determined by blood gases and respiratory mechanics; a final blinded echocardiogram and lung US study was performed at *Stabilization*. A stepwise inspired oxygen reduction test was performed obtaining serial arterial blood gases at each step. Pulmonary ventilation perfusion (V:Q) matching and intrapulmonary shunt fraction were calculated using software integrating established relationships between stepwise variations in FiO₂ and measured SaO₂, predicted for different levels of pulmonary shunt fraction (Qs/Qt) in human neonates.¹⁶

Animals were then euthanized by pentobarbital overdose. Heart and lungs were harvested en bloc. The right lung was inflation-fixed with 4% paraformaldehyde to functional residual capacity, using an

15 three-day-old piglets

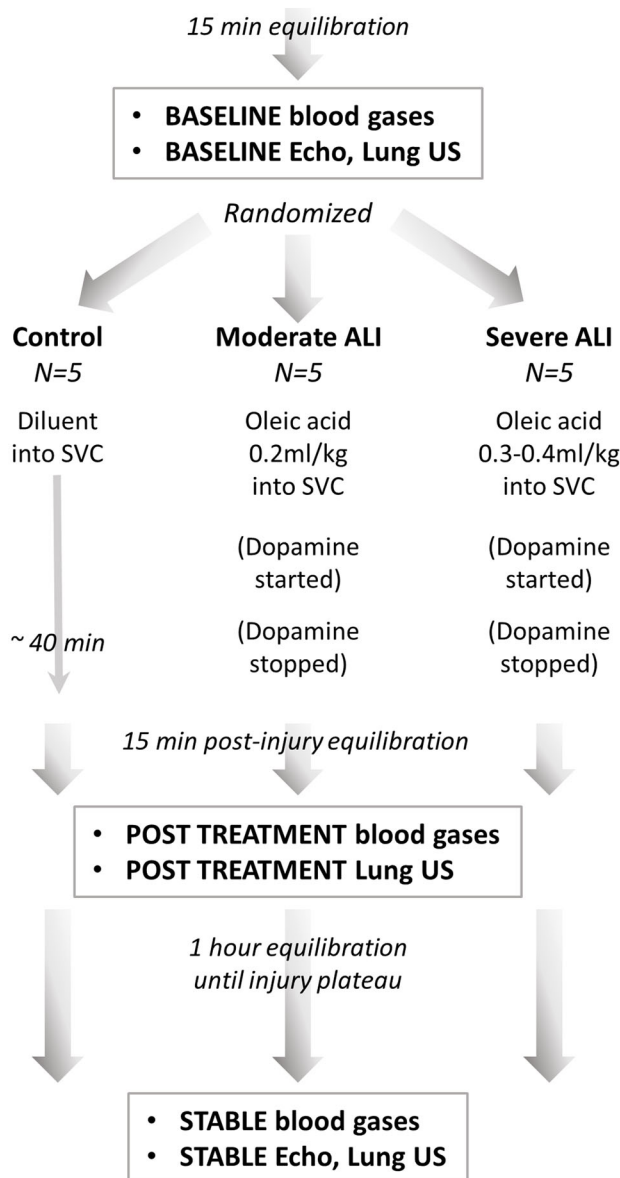
- Sedated, intubated 3.0 cuffed Ett
- Peripheral iv, maintenance fluids
- Anesthetized propofol/ketamine; paralyzed

Ventilation:

- AC VG 6ml/PEEP +6, FiO2 50%, Ti 0.3

Monitoring:

- Femoral arterial line
- Femoral venous line
- Internal jugular venous line
- Temperature probe
- Saturation monitor



Lung Ultrasound probe placement:

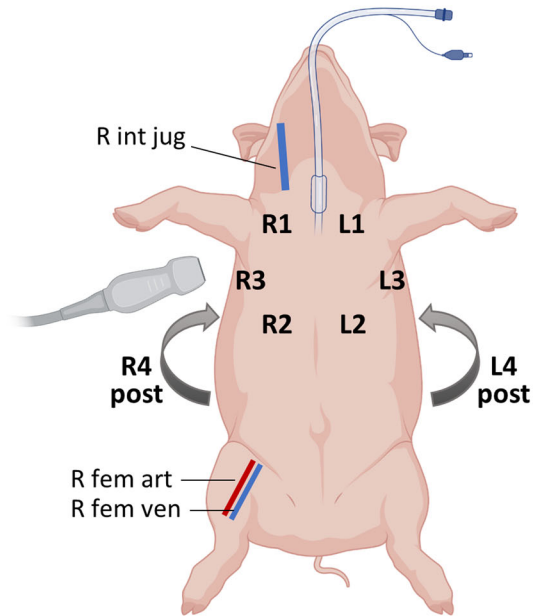


FIGURE 1 Study design flowchart. Data collection workflow for control, moderate injury, and severe oleic acid injury treatment groups. ALI, acute lung injury; Ett, endotracheal tube; SVC, superior vena cava [Color figure can be viewed at wileyonlinelibrary.com]

inflation pressure equal to the mean airway pressure measured at the end experiment. In anterior and posterior tissue sections from each lung, a composite histological lung injury score was calculated, following the American Thoracic Society Acute Lung Injury in Animals consensus method¹⁷; details provided in Methods supplement.

Data were analyzed by analysis of variance for repeated measures with Tukey correction for multiple comparisons, $P < .05$ considered significant. Linear regression modeling compared lung injury histological scores and intrapulmonary shunt to US scores.

3 | RESULTS

Fifteen 3-day-old piglets (60% male; average weight: 2.2 ± 0.1 kg) were randomized to control (sham infusion; $N = 5$), moderate lung injury ($N = 5$), or severe lung injury ($N = 5$). Baseline hemoglobin was low owing to iron-deficiency anemia common in farm-sourced piglets¹⁸ and was not different between groups; the homeostatic temperature was maintained in all groups.

3.1 | Hemodynamics

Tachycardia and hypotension developed in both OA injury groups posttreatment and increased in the severe group over time; progressively worsening hypotension developed in severe injury animals only. Central venous pressure remained stable in all groups during the observation period (Table 1).

3.2 | Functional echocardiography

Echocardiography revealed a decrease of both left and right ventricular cardiac outputs (Figure 2A,B), as well as a decrease in tricuspid annular plane systolic excursion (TAPSE; Figure 2C), in moderate and severe lung injury groups poststabilization. The most severe impairment was observed in right ventricular output. The ductus arteriosus was closed in most animals, and no animals demonstrated significant ductal shunting. Normalized pulmonary artery acceleration time (PAAT:ET; Figure 2D) was not significantly different between groups, nor were systolic or diastolic eccentricity indices (Figure 2E,F), largely due to very impaired cardiac filling and diminished cardiac output in both OA treatment groups limiting the utility of these measures of pulmonary pressure. Tricuspid regurgitation was not present, again reflecting poor right ventricular ejection fraction. Systemic vascular resistance (SVR; Figure 2G) was elevated in both OA injured groups.

3.3 | Ventilation parameters, gas exchange, and respiratory mechanics

Control animals exhibited stable PIP, PEEP, MAP, and minute ventilation during the ~3 hours of mechanical ventilation in the study

(Figure 3). PIP (Figure 3A) and MAP (Figure 3B) increased with OA lung injury, more significantly in the severe injury group. Only the severe injury animals required an increase in PEEP to maintain oxygenation with fixed FiO_2 50%.

Clinically apparent lung injury was determined from the analysis of pulmonary graphics. Static lung compliance (Figure 3E) decreased in moderate and to a greater extent in severe injury groups immediately posttreatment; dynamic compliance (C20/C; Figure 3F) trended lower after stabilization but did not reach significance, and time constant was unchanged (Figure 3G). Airway resistance (Figure 3H) increased only in the severe injury group at stabilization.

Moderate and severe groups had a progressive fall in pH (Figure 4A) and bicarbonate (Figure 4D), and a prompt drop in arterial PO_2 (Figure 4C). Arterial PCO_2 did not differ significantly between groups (Figure 4B). Moderately injured animals maintained oxygen saturation immediately post OA infusion, but desaturated to the same degree as severely injured animals by stabilization (Figure 4E).

To quantify oxygenation defects created by ALL, an alveolar-arterial difference (A-a diff) was calculated using the alveolar gas equation, and P/F ratio calculated as $\text{PaO}_2:\text{FiO}_2$, at the stabilized timepoint. Both the moderate and severe lung injury groups exhibited an A-a difference more than 150 mm Hg (Figure 4F), and a P/F ratio below 300 (Figure 4G). Control animals maintained a V:Q ratio around 0.7 after 3 hours mechanical ventilation; moderate injury decreased that ratio by half, and severe injury dropped the VQ ratio to less than a third that of controls (Figure 4H). The calculated intrapulmonary shunt fraction was well above 30% in both moderately and severely injured lungs (Figure 4I).

3.4 | POCUS and lung histology

There was no independent effect of mechanical ventilation on lung US scores in controls over the course of the experiment. Comparison of anterior lung US scores (cumulative score of 3 zones,

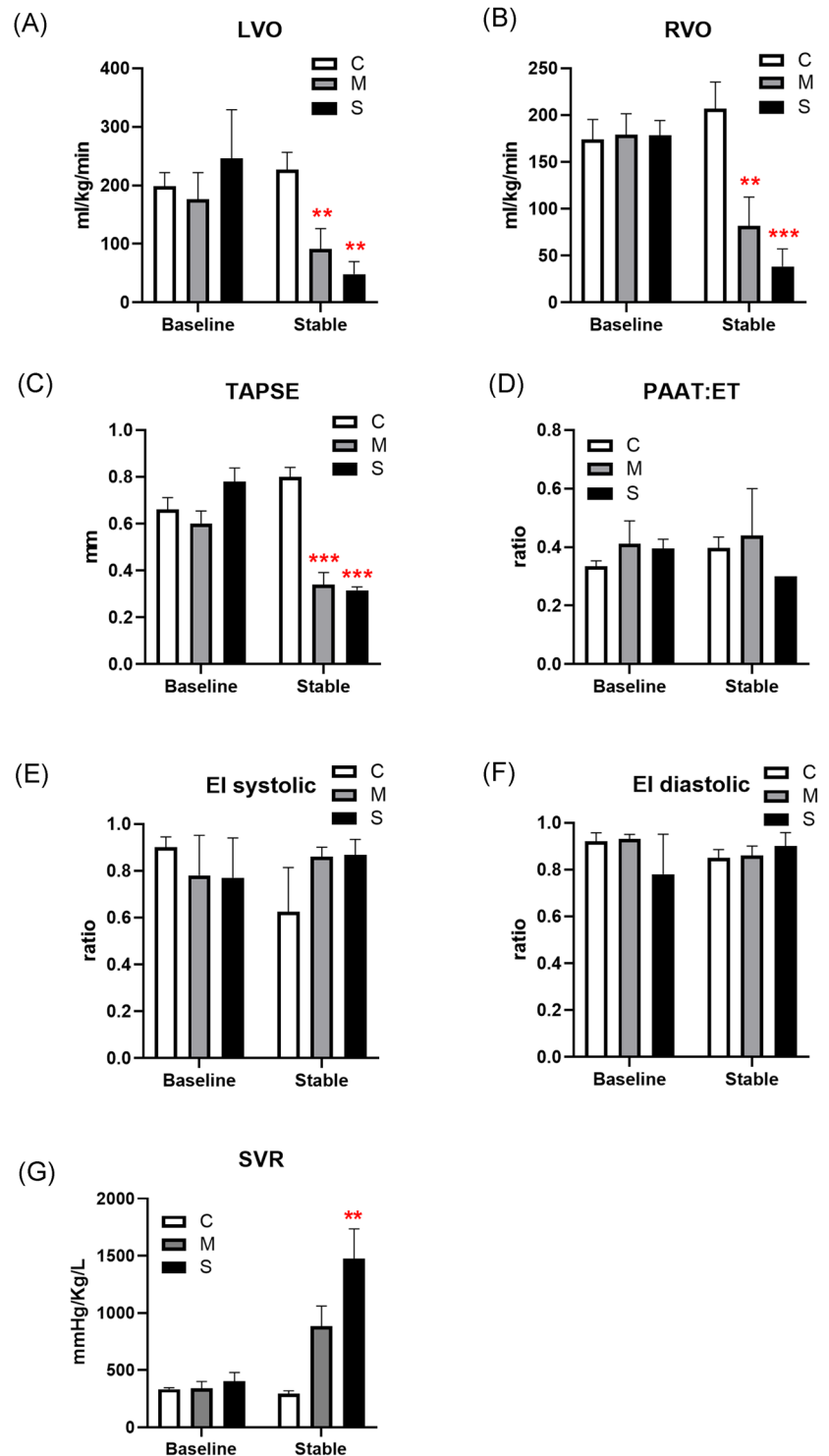
TABLE 1 Group characteristics

		Control	Moderate	Severe
HR	Baseline	142 ± 6	164 ± 9	177 ± 9*
	Post Tx	145 ± 7	192 ± 18	227 ± 26*
	Stable	150 ± 5	205 ± 13	236 ± 21**
MBP	Baseline	80.8 ± 3.4	69.5 ± 4.4	84.5 ± 5.6
	Post Tx	78.3 ± 2.1	68.4 ± 4.8	64.7 ± 7.2
	Stable	75.2 ± 3.9	68.8 ± 6.5	53.4 ± 5.6*
CVP	Baseline	8.8 ± 0.2	10.0 ± 1.1	8.2 ± 0.4
	Post Tx	8.8 ± 0.2	10.2 ± 1.5	7.0 ± 1.1
	Stable	9.0 ± 0.58	9.0 ± 0.84	8.0 ± 0.71

Note: Heart rate (HR, bpm), mean blood pressure (MBP, mm Hg), and central venous pressure (CVP) measured at baseline, 1 h posttreatment and at the stabilized timepoint at end of study, represented as mean ± SE for each group ($N = 5$).

* $P < .05$; ** $P < .01$ compared with the control group.

FIGURE 2 Hemodynamics by echocardiography. Cardiac left (LVO; A) and right (RVO; B) ventricular outputs, tricuspid annular plane systolic excursion (TAPSE; C), ratio of pulmonary artery acceleration time to ejection time (PAAT:ET; D), systolic (E), and diastolic (F) eccentricity indices (EI), and systemic vascular resistance (SVR; G) measured at baseline and at end of study, represented as mean ± SE for each group (N = 5; **P < .01, ***P < .001 compared with the control group) [Color figure can be viewed at wileyonlinelibrary.com]



max possible value = 9) at posttreatment and stable timepoints reproducibly distinguished between controls, moderate injury, and severe injury (Figure 5A). The degree of injury could also be discerned in each distinct anterior lung US zone (Figure 5Ai-iii). Posterior lung scores (1 zone, max value = 3; Figure 5B) were high and indistinguishable immediately posttreatment in both OA-treated groups. Cumulative lung US scores (combined anterior and

posterior scores) showed a dose-dependent worsening of OA lung injury over time (Figure 5C).

From histology, mechanical ventilation alone for the duration of the experiment did not create significant lung injury in controls. In both moderate and severe OA injury, marked lung injury (composite scores around 0.4) in both anterior and posterior lung was evident due to neutrophil infiltration, proteinaceous debris in alveolar spaces,

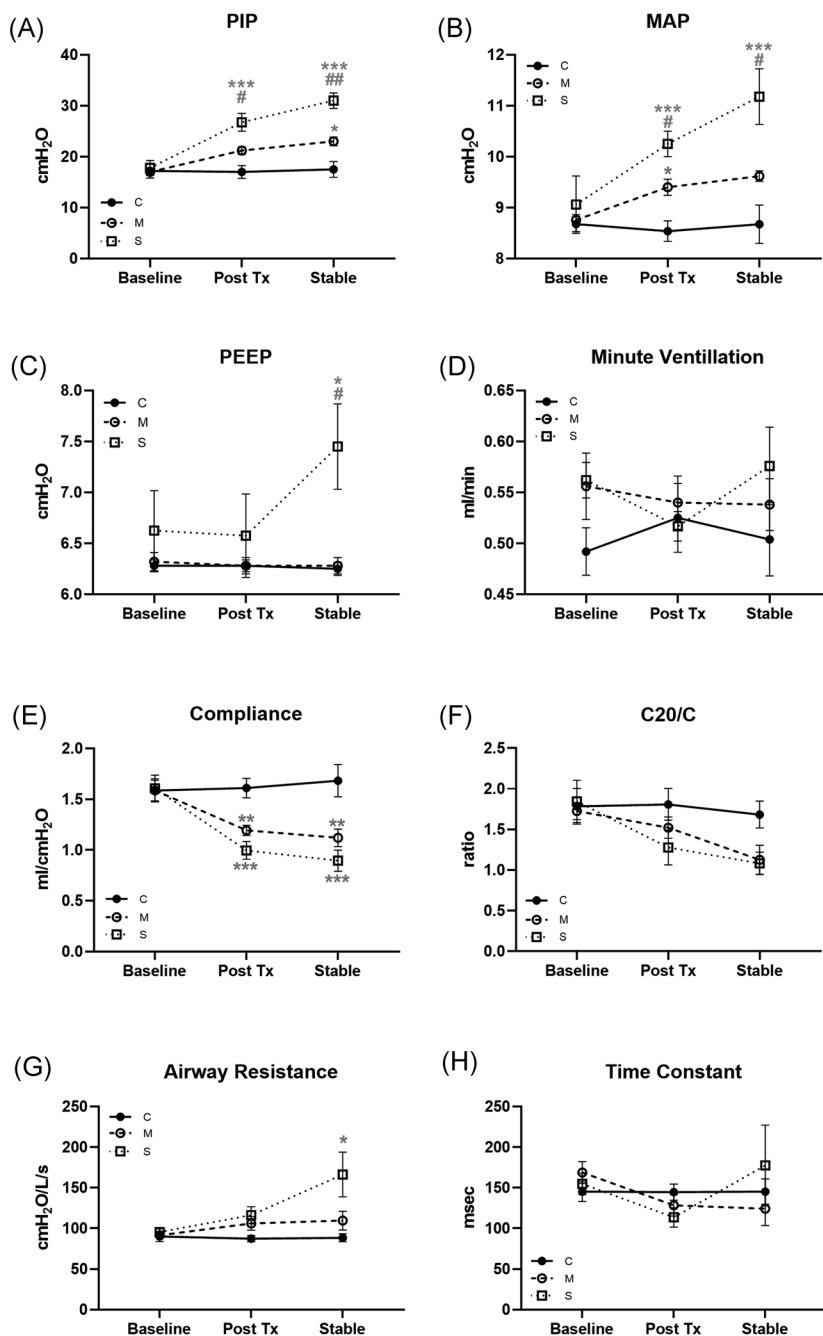


FIGURE 3 Ventilation parameters and clinical lung mechanics. A, Peak inspiratory pressure (PIP), (B) mean airway pressure (MAP), (C) positive end-expiratory pressure (PEEP), and (D) minute ventilation measured at baseline, 1 hour posttreatment and at end of study; represented as mean \pm SE for each group ($N = 5$; * $P < .05$, *** $P < .001$ compared with the control group; # $P < .05$, ## $P < .01$ compared with the moderate group). Compliance (E), C20/C index (F), airway resistance (G), and time constant (H) measured at baseline, 1 hour posttreatment and at end of study, represented as mean \pm SE for each group ($N = 5$; * $P < .05$, ** $P < .01$, *** $P < .001$ compared with the control group)

and thickening of alveolar walls. (Figure 6A,B). Histological injury scores plotted against cumulative US injury scores revealed clustering of controls versus all OA-treated animals, and correlation of the two lung injury scoring methods with $R^2 = .61$ (Figure 6C). As a physiological comparator, the correlation between US score and calculated intrapulmonary shunt fraction had $R^2 = .65$ (Figure 6D).

4 | DISCUSSION

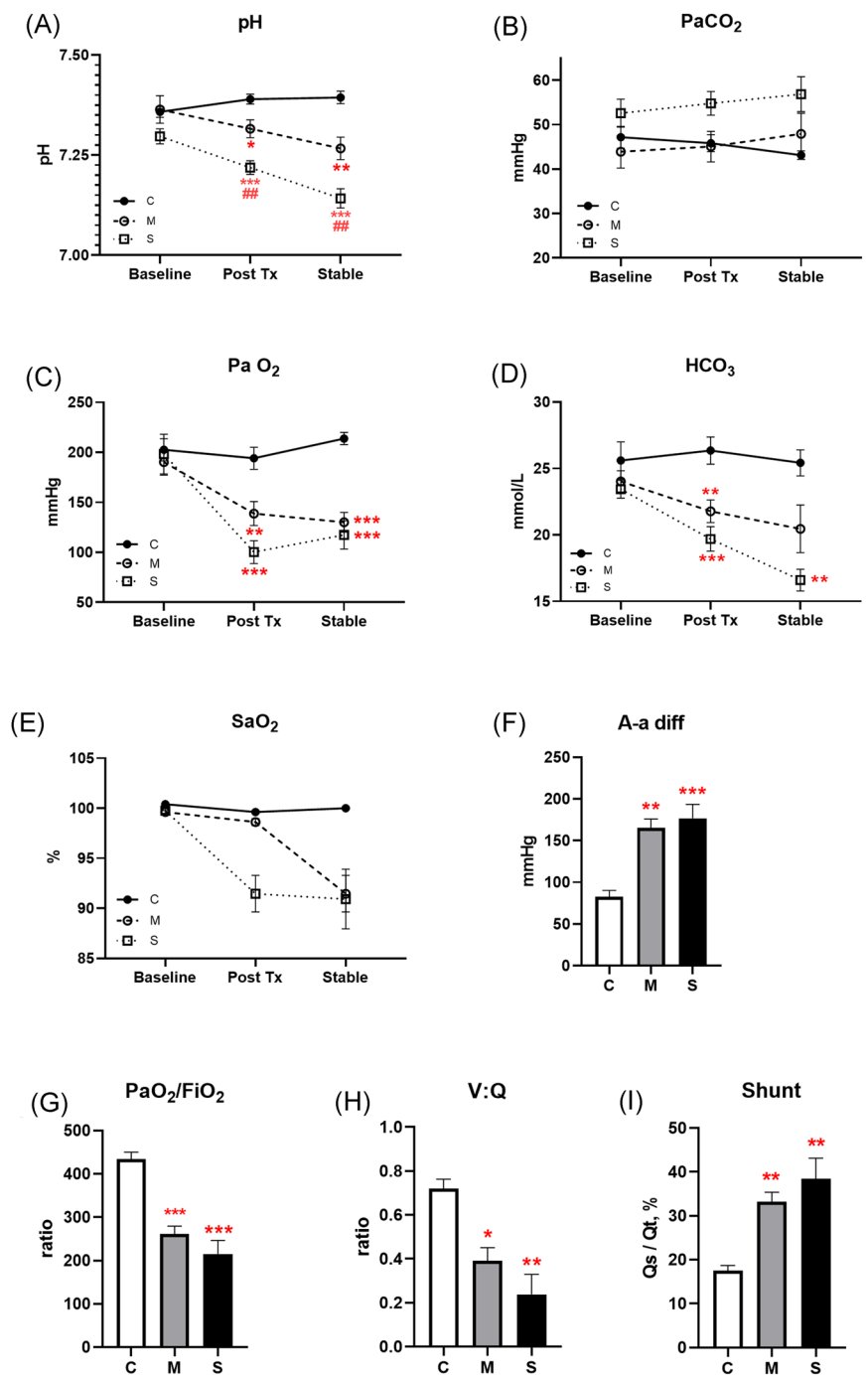
This is the first study to validate neonatal lung US against acute tissue injury using a standardized rubric, with attention to the value of

regional US scores. We tested the hypothesis that lung US is a sensitive indicator of ARDS, and would, therefore, correlate closely with canonical histological injury scores in an OA model of ALI in neonatal swine.

OA infusion induces morphologic and cellular changes similar to those observed in human ARDS.⁴ The evolution of OA-induced ALI can be evidenced by the appearance of normally impermeable infused dextran in bronchoalveolar lavage fluid within 30 minutes of OA treatment, peaking by 90 minutes posttreatment, followed by slow recovery of barrier function starting 2 hours posttreatment.¹⁹ Our observations were conducted at a plateau of endothelial injury.

Clinical indices of severity of ALI include decreased $\text{PaO}_2/\text{FiO}_2$ (P/F) ratio and loss of lung compliance.¹⁰ ALI and ARDS are

FIGURE 4 Blood gases and calculated lung injury. Arterial pH (A), PaCO₂ (B), PaO₂ (C), HCO₃ (D), and arterial oxygen saturation (SaO₂; E) measured at baseline, 1 hour posttreatment and at end of study, represented as mean ± SE for each group. Alveolar-arterial difference (A-a diff; F), ratio of PaO₂:FiO₂ (G), ventilation to perfusion ratio (V:Q, H) and intrapulmonary shunt fraction (I) calculated from measured parameters at end of study (N = 5; *P < .05, **P < .01, ***P < .001 compared with the control group; ##P < .01 compared with the moderate group) [Color figure can be viewed at wileyonlinelibrary.com]



distinguished by degree of hypoxemia; ALI is defined as having a P/F ratio less than 300, regardless of PEEP level; ARDS as P/F less than 200.²⁰ By these criteria, animals in our moderate injury group would be categorized as ALI, while the severe injury group approached the more stringent definition of ARDS. We also calculated the alveolar-arterial (A-a) PO₂ difference, an indicator of diffusion gradient reflecting alveolar filling; while just the duration of mechanical ventilation did increase A-a difference in the control group above the normal range (< 10 mm Hg), both OA-treated groups had A-a differences well into the pathological range.

Lung mechanics were derived from ventilator pressure-volume loops, which in lung injury models surpass oxygenation indices in predicting alveolar recruitment.²¹ Inspiratory pressure and mean airway pressure required to deliver a set TV increased quickly in the severe injury group, but more modestly in the moderate injury group; only severe injury animals required an increase in PEEP to maintain adequate oxygenation. Quasi-static compliance of the respiratory system was calculated from measured tissue elastance.²² During postnatal adaptation while lung water is resorbed, static compliance improves as ultrasonographically detected B-lines regress,²³ making

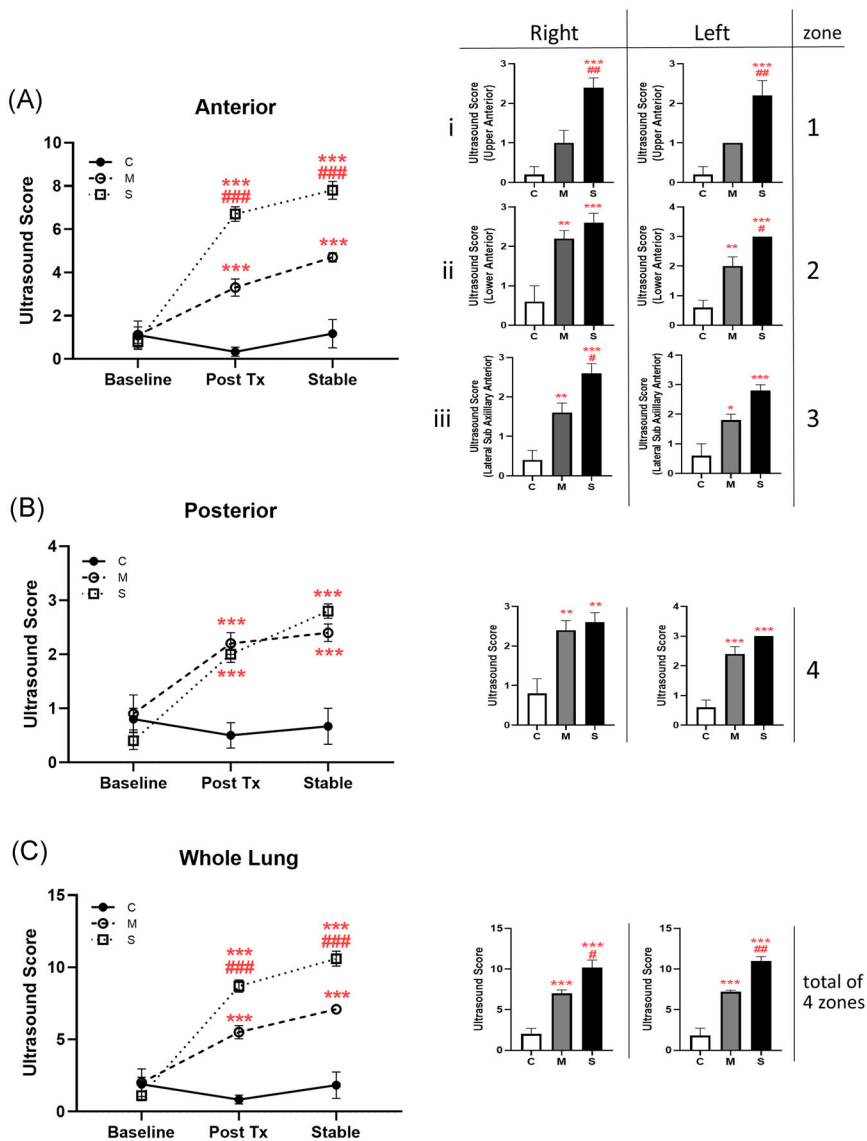


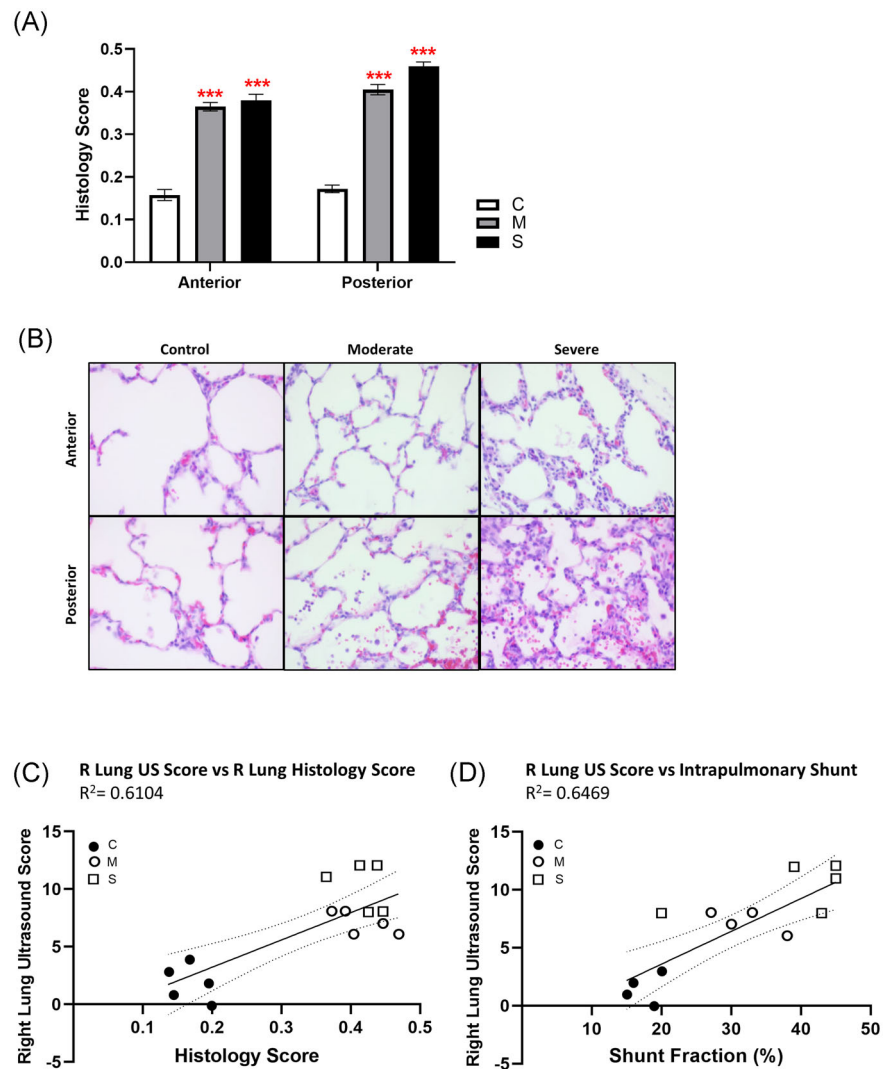
FIGURE 5 Ultrasound lung injury score. Ultrasound images captured at baseline, 1 hour posttreatment and at end of study; scores are represented as mean \pm SE for each group. Anterior measurements (A) are cumulative values obtained from (i) upper, (ii) lower, and (iii) lateral zones; posterior values (B) obtained from a single posterolateral zone per lung. (C) Total lung ultrasound score is the sum of anterior (three zones) and posterior (one zone) images per lung. Histograms show the measurement at the stabilized timepoint for individual zones studied. ($N = 5$; * $P < .05$, ** $P < .01$, *** $P < .001$ compared with the control group; # $P < .05$, ## $P < .01$, ### $P < .001$ compared with the moderate group) [Color figure can be viewed at wileyonlinelibrary.com]

a loss of compliance a pertinent marker of lung water in this study. We observed significant compliance loss in both moderate and severe lung injury, worsening over the time course of the study. On the other hand, loss of dynamic compliance (ratio of compliance of the upper 20% of the P/V curve to total compliance, or $C_{20}/C < 0.8$) can reflect overdistension of the lung.²⁴ C_{20}/C trended downward but was not significantly decreased in OA-treated groups, indicating that any changes we observed in cardiac output or pulmonary vascular mechanics could not be ascribed to pulmonary overinflation.²⁵ The time constant (TC), the time required for the lung unit to fill or empty was unchanged in OA-treated groups suggesting the applied PEEP was adequate to mitigate end-expiratory resistance.²⁶ ARDS is known to cause TC heterogeneities resulting in inhomogenous aeration of lung regions, which may explain wider error bars obtained in these data.

The hallmark of OA injury is an abrupt and profound capillary leak, shifting intravascular fluid into the alveoli space. We observed

marked decreases in cardiac left and right ventricular outputs, with much diminished diastolic filling consistent with loss of intravascular volume. Measured CVP was unchanged, a less sensitive indicator if circuit pressure is maintained evident from the associated increase in calculated SVR. SVR elevation following OA injury has been reported previously, presumably reflecting reflex adrenergic activation.²⁷ Increased pulmonary artery pressure and pulmonary vascular resistance are well documented with OA administration in older porcine models whose size permits direct placement of a pulmonary arterial catheter. In the neonatal OA model, echocardiographic eccentricity indices and PAAT:ejection time ratio (PAAT:ET; a flow-sensitive indicator of pulmonary vascular resistance) served as alternatives. These indices were unchanged due to profound right ventricular dysfunction manifested by decreased TAPSE. Attenuated PAAT:ET in RV failure with decreased TAPSE has been reported in models of pulmonary hypertension.²⁸ As such, we are unable to comment specifically upon pulmonary vascular hemodynamics in this

FIGURE 6 Histological lung injury score. Hematoxylin/eosin-stained 0.6 μm -thick sections from anterior and posterior lung tissue blocks from the inflation-fixed right lung of each animal were scored for presence of [a] neutrophils in alveolar space; [b] neutrophils in interstitial space; [c] hyaline membranes; [d] proteinaceous debris in airspaces; and [e] alveolar septal thickening, and reported as a composite histological lung injury score = $[(20 \times a) + (14 \times b) + (7 \times c) + (7 \times d) + (2 \times e)] / (\text{number of fields} \times 100)$ (A). ($N = 5$; $***P < .001$ compared with the control group). Representative images from anterior and posterior tissue sections shown (B). Ultrasound score calculated for right lung compared with (C) right lung composite histology score and (D) calculated intrapulmonary shunt, by linear regression with 95% confidence interval denoted by the dashed line (both slopes indicate significant correlation, $P < .01$) [Color figure can be viewed at wileyonlinelibrary.com]



study. However, right ventricular output was more impaired than left, possibly due in part to right-to-left shunting via the foramen ovale in face of high right-sided afterload.

Blood gases were more rapidly altered in severe injury animals, the falling pH reflecting impaired perfusion without a significant change in respiratory acidosis. PaO_2 decreased immediately after OA treatment in both moderate and severe injuries. Oxygen saturation was initially maintained in the moderate injury group but fell by the end of the study. This discrepancy between PaO_2 and SaO_2 may be explained by the less severe impairment in calculated V:Q matching in the moderate injury group. The hypoxemia that characterizes ARDS is ascribed primarily to intrapulmonary shunting, with V:Q matching preserved until a severe injury, when perfusion of low V:Q regions contributes to hypoxemia.²⁹ Intrapulmonary shunt fraction was significantly increased in both OA-treated groups. Intrapulmonary shunt, A-a difference, mean airway pressure and PaO_2 (but not SaO_2) have been shown to correlate linearly with the severity of lung edema in ALI.³⁰

Lung US has been proposed as a valid alternative to chest radiography or CT to diagnose ARDS in the adult population³¹; but the

pediatric and neonatal experience is limited.¹³ In OA injury models, vertical hyperechoic B-lines correlating with increasing extravascular lung water are detectable starting 15 minutes after OA injury, coincident with the fall in static pulmonary compliance but before onset of functional impairments such as hypoxemia or decreased P/F ratio.³² A semi-quantitative 6-region lung US scoring index was originally developed in septic adults for early identification of pulmonary edema³³; we utilized a modified version validated for neonatal lung disease.³⁴ Anterior lungs were divided into upper, lower, and lateral zones; however, the posterior lung was assessed in a single posterolateral zone, as animals were maintained in the supine position, based on our previous report that change to prone position mid-study would require a subsequent 1 hour restabilization period.³⁵ In each zone, a US score of 0 = only horizontal A-lines; 1 = less than or equal to 3 well-spaced B-lines; 2 = crowded B-lines and/or subpleural consolidation; 3 = extended subpleural consolidation more than 1 cm, for a maximum US score of 24 for each animal. Due to the known heterogeneity of ALI, we also compared scores for each zone. We found that moderate and severe lung injury were indistinguishable in dependent regions, but anterior US scores and cumulative scores clearly separated moderate

from severe groups and increased from initial injury over 1 hour suggesting an ability to track injury progression. In ARDS, earliest US abnormalities appear in posterior regions, with a most rapid filling of dependent alveoli³⁶; our data confirm this, and we propose that once lung edema is detected in dependent areas in early ARDS, anterior views may be more useful for tracking progression and grading ARDS severity while in the supine position. This corroborates findings in adult patients with ARDS,³⁷ and also in coronavirus disease-2019-related ARDS.³⁸ X-ray has been presumed superior to the US in the diagnosis of ARDS due to deeper posterior penetration of the former in a predominantly posterior disease.³⁶ Although we were unable to compare the US to chest X-rays in this study, the finding that the easily-accessed anterior lung US zones reveal early ARDS progression may call this assumption into question.

Postmortem removal of the lungs after 3 hours of mechanical ventilation revealed that control lungs appeared grossly normal with only mild basal erythema; lungs of both moderate and severe groups appeared engorged, ruddy, and hemorrhagic. Histologic quantification of lung injury in anterior and posterior lung tissue was similar for moderate and severe groups; however, in each discrete category of grading,¹⁷ severely injured lungs were qualitatively at the upper end of the range with greater membrane thickening, more visible alveolar debris and more neutrophilic infiltration than moderately injured lung. Comparisons of composite lung US score in stabilized lung injury with histopathologic score (both measured in right lung) indicate a moderate degree of correlation between in vivo US observation and the gold standard for degree of tissue injury. A recent study of OA-induced ALI in adult rabbits compared the US obtained ex vivo with tissue histology, finding the frequency of postmortem B-line artifact correlates closely with the severity of lung pathologic abnormalities in each regional lung segment.³⁹ That study used a semi-quantitative 4-point grading system, in conjunction with serum inflammatory markers. Using the American Thoracic Society's consensus method for ALI histology and a premortem POCUS score, we report that the US score predicts the magnitude of tissue injury. This correlation holds even in moderate ALI where early preservation of V:Q matching may blunt some clinical indicators of hypoxemia, risking an underestimation of ALI severity assessed by clinical parameters alone. We also report US score correlation with ALI-induced intrapulmonary shunt fraction, an important clinical measure of injury severity.

Limitations include the small number of animals studied and the 3 hour timeframe of the experiment; as others have reported,³ we were constrained by morbidity and mortality in the severe lung injury group and could not reliably maintain hemodynamic stability for a longer observation period. The utility of the US to track the evolution of ARDS over longer time periods, and to evaluate the benefits of specific treatment modalities in the neonate, warrants further study.

In summary, we have developed a reproducible neonatal lung injury model at two levels of lung injury manifested by distinct lung mechanics, blood gases, intrapulmonary shunt, and US imaging. Although comparison of the US against a histological standard is reported ex vivo in adult models,^{39,40} this is the first to report a significant correlation in a neonatal model, imaged in vivo. The results

suggest that POCUS is a potentially useful imaging modality in neonates with suspected ALI or ARDS, to diagnose and track the evolution of lung injury. The combination of lung US and functional echocardiography provide a more complete picture of the cardiopulmonary consequences of neonatal ARDS and may aid in management.

ACKNOWLEDGMENTS

We gratefully acknowledge technical assistance by Faraz Ahmed and Jacquie Schwartz. Statistics used GraphPad Prism software; graphics created with BioRender.com. The study was supported by grants from University of Manitoba Department of Anesthesia Peri-operative and Pain Medicine (MRG), Winnipeg Rh Institute Foundation (MRG, YE), and Heart and Stroke Foundation of Canada (SD) (G190024330).

CONFLICT OF INTERESTS

No financial ties or conflicts of interest to disclose.

AUTHOR CONTRIBUTIONS

YE and MRG designed and performed experiments, analyzed results, and contributed to the manuscript. MH designed and performed experiments, analyzed results, and designed figures. SD designed experiments, analyzed results, and finalized the manuscript.

ORCID

Shyamala Dakshinamurti  <http://orcid.org/0000-0001-7279-5226>

REFERENCES

1. Singh Y, Tissot C, Fraga MV, et al. International evidence-based guidelines on Point of Care Ultrasound (POCUS) for critically ill neonates and children issued by the POCUS Working Group of the European Society of Paediatric and Neonatal Intensive Care (ESP-NIC). *Crit Care*. 2020;24(1):65.
2. Tisoncik JR, Korth MJ, Simmons CP, Farrar J, Martin TR, Katze MG. Into the eye of the cytokine storm. *Microbiol Mol Biol Rev*. 2012;76(1):16-32.
3. Uhlig S, Kuebler WM. Difficulties in modelling ARDS (2017 Grover Conference Series). *Pulm Circ*. 2018;8(2):2045894018766737.
4. Matute-Bello G, Frevert CW, Martin TR. Animal models of acute lung injury. *Am J Physiol Lung Cell Mol Physiol*. 2008;295(3):L379-L399.
5. Beilman G. Pathogenesis of oleic acid-induced lung injury in the rat: distribution of oleic acid during injury and early endothelial cell changes. *Lipids*. 1995;30(9):817-823.
6. Graham MR, Haberman CJ, Brewster JF, Girling LG, McManus BM, Mutch WA. Mathematical modelling to centre low tidal volumes following acute lung injury: a study with biologically variable ventilation. *Respir Res*. 2005;6:64.
7. Graham MR, Gulati H, Kha L, Girling LG, Goertzen A, Mutch WA. Resolution of pulmonary edema with variable mechanical ventilation in a porcine model of acute lung injury. *Can J Anaesth*. 2011;58(8):740-750.
8. Moodley Y, Sturm M, Shaw K, et al. Human mesenchymal stem cells attenuate early damage in a ventilated pig model of acute lung injury. *Stem Cell Res*. 2016;17(1):25-31.
9. Ruth Graham M, Goertzen AL, Girling LG, et al. Quantitative computed tomography in porcine lung injury with variable versus conventional ventilation: recruitment and surfactant replacement. *Crit Care Med*. 2011;39(7):1721-1730.
10. De Luca D, van Kaam AH, Tingay DG, et al. The Montreux definition of neonatal ARDS: biological and clinical background behind the description of a new entity. *Lancet Respir Med*. 2017;5(8):657-666.

11. Pisani L, Riviello ED, Schultz MJ. Lung ultrasound and neonatal ARDS: is Montreux closer to Berlin than to Kigali? *Lancet Respir Med*. 2017; 5(11):e31.
12. De Luca D, van Kaam AH, Tingay DG, et al. Lung ultrasound and neonatal ARDS: is Montreux closer to Berlin than to Kigali? - Authors' reply. *Lancet Respir Med*. 2017;5(11):e32.
13. Potter SK, Griksaitis MJ. The role of point-of-care ultrasound in pediatric acute respiratory distress syndrome: emerging evidence for its use. *Ann Transl Med*. 2019;7(19):507.
14. Amer R, Elsayed YN, Graham MR, Sikarwar AS, Hinton M, Dakshinamurti S. Effect of vasopressin on a porcine model of persistent pulmonary hypertension of the newborn. *Pediatr Pulmonol*. 2019;54(3):319-332.
15. Abdelmawla M, Louis D, Narvey M, Elsayed Y. A lung ultrasound severity score predicts chronic lung disease in preterm infants. *Am J Perinatol*. 2019;36(13):1357-1361.
16. Smith HL, Jones JG. Non-invasive assessment of shunt and ventilation/perfusion ratio in neonates with pulmonary failure. *Arch Dis Child Fetal Neonatal Ed*. 2001;85(2):F127-F132.
17. Matute-Bello G, Downey G, Moore BB, et al. An official American Thoracic Society workshop report: features and measurements of experimental acute lung injury in animals. *Am J Respir Cell Mol Biol*. 2011;44(5):725-738.
18. Perri AM, Friendship RM, Harding JSC, O'Sullivan TL. An investigation of iron deficiency and anemia in piglets and the effect of iron status at weaning on post-weaning performance. *J Swine Health Prod*. 2016; 24(1):10-20.
19. Briot R, Bayat S, Anglade D, Martiel JL, Grimbert F. Monitoring the capillary-alveolar leakage in an A.R.D.S. model using broncho-alveolar lavage. *Microcirculation*. 2008;15(3):237-249.
20. Bernard GR, Artigas A, Brigham KL, et al. The American-European Consensus Conference on ARDS. Definitions, mechanisms, relevant outcomes, and clinical trial coordination. *Am J Respir Crit Care Med*. 1994;149(3 Pt 1):818-834.
21. Koefoed-Nielsen J, Nielsen ND, Kjaergaard AJ, Larsson A. Alveolar recruitment can be predicted from airway pressure-lung volume loops: an experimental study in a porcine acute lung injury model. *Crit Care*. 2008;12(1):R7.
22. Larsson A, Guerin C. Monitoring of lung function in acute respiratory distress syndrome. *Ann Transl Med*. 2017;5(14):284.
23. Martelius L, Suvvari L, Janér C, et al. Lung ultrasound and static lung compliance during postnatal adaptation in healthy term infants. *Neonatology*. 2015;108(4):287-292.
24. Nève V, de la Roque ED, Leclerc F, et al. Ventilator-induced overdistension in children: dynamic versus low-flow inflation volume-pressure curves. *Am J Respir Crit Care Med*. 2000;162(1): 139-147.
25. Cheifetz IM, Craig DM, Quick G, et al. Increasing tidal volumes and pulmonary overdistention adversely affect pulmonary vascular mechanics and cardiac output in a pediatric swine model. *Crit Care Med*. 1998;26(4):710-716.
26. Kondili E, Prinianakis G, Athanasakis H, Georgopoulos D. Lung emptying in patients with acute respiratory distress syndrome: effects of positive end-expiratory pressure. *Eur Respir J*. 2002;19(5):811-819.
27. Sum-Ping ST, Symreng T, Jebson P, Kamal GD. Stable and reproducible porcine model of acute lung injury induced by oleic acid. *Crit Care Med*. 1991;19(3):405-408.
28. Zhu Z, Godana D, Li A, et al. Echocardiographic assessment of right ventricular function in experimental pulmonary hypertension. *Pulm Circ*. 2019;9(2):2045894019841987.
29. Sinclair SE, Albert RK. Altering ventilation-perfusion relationships in ventilated patients with acute lung injury. *Intensive Care Med*. 1997; 23(9):942-950.
30. Chiang CH, Shen CY, Hsu K. Correlation between cardiopulmonary changes and severity of acute lung injury in dogs. *Crit Care Med*. 1990; 18(4):419-422.
31. Pesenti A, Musch G, Lichtenstein D, et al. Imaging in acute respiratory distress syndrome. *Intensive Care Med*. 2016;42(5):686-698.
32. Gargani L, Lionetti V, Di Cristofano C, Bevilacqua G, Recchia FA, Picano E. Early detection of acute lung injury uncoupled to hypoxemia in pigs using ultrasound lung comets. *Crit Care Med*. 2007;35(12):2769-2774.
33. Santos TM, Franci D, Coutinho CM, et al. A simplified ultrasound-based edema score to assess lung injury and clinical severity in septic patients. *Am J Emerg Med*. 2013;31(12):1656-1660.
34. Brat R, Yousef N, Klifa R, Reynaud S, Shankar Aguilera S, De Luca D. Lung ultrasonography score to evaluate oxygenation and surfactant need in neonates treated with continuous positive airway pressure. *JAMA Pediatrics*. 2015;169(8):e151797.
35. Louis D, Belen K, Farooqui M, et al. Prone versus supine position for lung ultrasound in neonates with respiratory distress [published online ahead of print September 3, 2019]. *Am J Perinatol*. 2019. <https://doi.org/10.1055/s-0039-1695776>
36. See KC, Ong V, Tan YL, Sahagun J, Taculod J. Chest radiography versus lung ultrasound for identification of acute respiratory distress syndrome: a retrospective observational study. *Crit Care*. 2018;22(1):203.
37. Pisani L, Vercesi V, van Tongeren PSI, et al. The diagnostic accuracy for ARDS of global versus regional lung ultrasound scores - a post hoc analysis of an observational study in invasively ventilated ICU patients. *Intensive Care Med Exp*. 2019;7(suppl 1):44.
38. Kulkarni S, Down B, Jha S. Point-of-care (POC) lung ultrasound in intensive care during the COVID-19 pandemic [published online ahead of print May 13, 2020]. *Clin Radiol*. 2020. <https://doi.org/10.1016/j.crad.2020.05.001>
39. Zhu Z, Lian X, Zeng Y, et al. Point-of-care ultrasound-a new option for early quantitative assessment of pulmonary edema. *Ultrasound Med Biol*. 2020;46(1):1-10.
40. Soldati G, Inchingolo R, Smargiassi A, et al. Ex vivo lung sonography: morphologic-ultrasound relationship. *Ultrasound Med Biol*. 2012;38(7): 1169-1179.

SUPPORTING INFORMATION

Additional supporting information may be found online in the Supporting Information section.

How to cite this article: Elsayed YN, Hinton M, Graham R, Dakshinamurti S. Lung ultrasound predicts histological lung injury in a neonatal model of acute respiratory distress syndrome. *Pediatric Pulmonology*. 2020;55:2913-2923. <https://doi.org/10.1002/ppul.24993>